Title: Simultaneous knockout of VITAMIN C DEFECTIVE 2 and 3 exacerbates ascorbate deficiency and light stress sensitivity

Running title: Functional and genetic relationship between VTC2 and VTC3

Authors: Yasuhiro Tanaka[1,2,†], Takanori Maruta[1,2,3,4,†,*], Koki Arima[3], Hiroki Nakayama[3], Akane Hamada[1,2], and Takahiro Ishikawa[1,2,3,4]

Affiliations:

[1] Graduate School of Natural Science and Technology, Shimane University, 1060 Nishikawatsu, Matsue, Shimane 690-8504, Japan

[2] Bioresource and Life Sciences, The United Graduate School of Agricultural Sciences, Tottori University, 4-101 Koyama-Minami, Tottori, Tottori 680-8553, Japan

[3] Department of Life Sciences, Faculty of Life and Environmental Science, Shimane University, 1060 Nishikawatsu, Matsue, Shimane 690-8504, Japan

[4] Institute of Agricultural and Life Sciences, Academic Assembly, Shimane University, 1060 Nishikawatsu, Matsue, Shimane 690-8504, Japan

[†] These authors contributed equally to the article.

[*] Corresponding author

Abstract

Light-dependent activation of ascorbate biosynthesis is essential for accumulating ascorbate to mitigate photooxidative stress. The *VTC2* and *VTC3* genes play key roles in this process: *VTC2* encodes GDP-L-galactose phosphorylase (GGP), the rate-limiting enzyme in ascorbate biosynthesis, and *VTC3* encodes a putative protein kinase/phosphatase with an unknown function. Here, we investigated their functional and genetic relationship. In *vtc3* mutants, *VTC2* transcription and GGP activity were slightly enhanced, suggesting that VTC3 is not required for VTC2 expression. Additionally, the *vtc3* mutation had negligible effects on the transcriptome and the activity of enzymes involved in ascorbate redox cycle regulation, narrowing down the possible roles of VTC3 in ascorbate biosynthesis. Under low-light conditions, ascorbate levels were lower in *vtc2* than in *vtc3* mutants, but *vtc2* retained the ability to increase ascorbate levels under high-light stress, unlike *vtc3*. The simultaneous knockout of VTC2 and VTC3 further reduced ascorbate levels compared to single mutants and severely impaired light stress-induced ascorbate accumulation, resulting in impaired non-photochemical quenching and enhanced photooxidative damage. These findings highlight the additive effects of VTC2 and VTC3 on ascorbate biosynthesis and stress tolerance. The *vtc2 vtc3* double mutants provide a valuable model for further elucidating the physiological roles of ascorbate in plants.

Keywords: Arabidopsis thaliana, ascorbate biosynthesis, GDP-L-galactose phosphorylase, high light, oxidative stress, vitamin C-defective

Abbreviations: APX, ascorbate peroxidase; ASC, ascorbate; DHA, dehydroascorbate; DHAR, dehydroascorbate reductase; GGP, GDP-L-galactose phosphorylase; GME, GDP-D-mannose-3',5'-epimerase; GMP, GDP-D-mannose pyrophosphorylase; GPP, L-galactose-1-phosphate phosphatase; GSH, reduced glutathione; L-GalDH, L-galactose dehydrogenase; L-GalLDH, L-galactono-1,4-lactone dehydrogenase; MDHA, monodehydroascorbate; MDAR, monodehydroascorbate reductase; NPQ, non-photochemical quenching; PMI, phosphomannose isomerase; PMM, phosphomannomutase; PP2C, protein phosphatase 2C; ROS, reactive oxygen species; uORF, upstream open reading frame; VTC, vitamin c defective

Introduction

In plants, reactive oxygen species (ROS) can be generated as byproducts of photosynthesis (Asada, 1999). Other major sources of ROS include the mitochondrial electron transport chain and the oxidation of glycolate in peroxisomes during photorespiration (Mittler *et al.*, 2022). In addition, plants possess multiple apoplastic ROS-producing enzymes, particularly NADPH oxidases (also known as respiratory burst oxidase homologs) (Mittler *et al.*, 2022). Under stress conditions, ROS generation through these various pathways is often inevitably increased or actively promoted as part of the plant's response mechanisms. While ROS are highly reactive and can damage cellular components at elevated levels, they also serve as critical signaling molecules in plant stress acclimation (Mittler *et al.*, 2022). Maintaining ROS homeostasis is essential for harnessing their signaling functions without compromising cellular integrity. This balance is achieved through robust antioxidant systems, among which ascorbate is one of the most abundant soluble antioxidants in plant leaves, present in all intracellular compartments at millimolar (mM) concentrations (Zechmann *et al.*, 2011; Smirnoff, 2018; Maruta *et al.*, 2024). Ascorbate plays a central role in scavenging ROS through both direct nonenzymatic reactions and enzymatic pathways mediated by ascorbate peroxidase (APX), an enzyme specific to eukaryotic photosynthetic organisms (Shigeoka *et al.*, 2002; Maruta *et al.*, 2016). Additionally, ascorbate serves as a substrate for violaxanthin de-epoxidase, an enzyme crucial for the xanthophyll cycle, which dissipates excess light energy as heat and limits ROS production during photosynthesis (Müller-Moulé *et al.*, 2004). Beyond its role in ROS management, ascorbate is involved in diverse biological processes, including photosynthetic electron transport, iron uptake, cell division, anthocyanin accumulation, and hormone biosynthesis (Smirnoff, 2018).

Several pathways for ascorbate biosynthesis have been proposed; however, the D-mannose/L-galactose (D-Man/L-Gal) pathway, also known as the Smirnoff–Wheeler pathway, is widely recognized as the primary route (Wheeler *et al.*, 1998; Smirnoff, 2018; Maruta, 2022). This notion is supported by substantial experimental evidence demonstrating its involvement in ascorbate biosynthesis across land plants and algae (Wheeler *et al.*, 1998; Conklin *et al.*, 1999; Vidal-Meireles *et al.*, 2017; Sodeyama *et al.*, 2021; Ishida *et al.*, 2024). The D-Man/L-Gal pathway synthesizes ascorbate from the hexose phosphate pool through eight enzymatic reactions catalyzed sequentially by phosphomannose isomerase (PMI), phosphomannomutase (PMM), GDP-D-mannose pyrophosphorylase (GMP), GDP-D-mannose-3',5'-epimerase (GME), GDP-L-galactose phosphorylase (GGP), L-galactose-1-phosphate phosphatase (GPP), L-galactose dehydrogenase (L-GalDH), and L-galactono-1,4-lactone dehydrogenase (L-GalLDH) (Smirnoff, 2018). The final step, catalyzed by L-GalLDH, occurs in the inner mitochondrial membrane, whereas all other enzymatic

steps take place in the cytosol (Smirnoff, 2018). The significance of the D-Man/L-Gal pathway has been confirmed mainly through the characterization of Arabidopsis vitamin C-defective (*vtc*) mutants. The genes *VTC1*, *VTC2*, and *VTC4* encode GMP, GGP, and GPP, respectively (Conklin *et al.*, 1999, 2006; Jander *et al.*, 2002; Laing *et al.*, 2007; Linster *et al.*, 2007). Arabidopsis also possesses a minor isoform of GGP, encoded by *VTC5*. Notably, a double knockout mutant of *VTC2* and *VTC5* results in undetectable ascorbate levels and exhibits seedling lethality unless supplemented with ascorbate or its precursors (Dowdle *et al.*, 2007).

Light is a potent stimulus for increasing the ascorbate pool size in plants. Leaf ascorbate content rises in response to light intensity and exposure duration (Dowdle *et al.*, 2007; Yabuta *et al.*, 2007). The key enzyme regulating ascorbate content under light conditions is VTC2/GGP, whose transcription is induced by light (Dowdle *et al.*, 2007; Yabuta *et al.*, 2007). Interestingly, the light-dependent activation of *VTC2* transcription is suppressed by photosynthesis inhibitors, suggesting a role for photosynthesis in the regulation of ascorbate biosynthesis (Yabuta *et al*., 2007). GGP activity is significantly enhanced under high-light stress, whereas the activities of other biosynthetic enzymes remain unaffected (Dowdle *et al*., 2007). Moreover, overexpression of VTC2 effectively enhances ascorbate pool sizes in various plant species (Bulley *et al.*, 2009, 2012; Yoshimura *et al.*, 2014). These findings confirm that VTC2/GGP is the rate-limiting enzyme in the D-Man/L-Gal pathway, a conclusion further supported by computational simulations (Fenech *et al.*, 2021). The regulation of VTC2 by light also occurs at the post-translational level. In the dark, GGP activity is inhibited by a new class of blue-light receptors, PAS/LOV proteins, which directly associate with GGP (Ogura *et al.*, 2008; Aarabi *et al.*, 2023; Bournonville *et al.*, 2023). Upon exposure to blue light, PAS/LOV proteins are dissociated from GGP, promoting its enzymatic activity. Thus, light-dependent activation of GGP plays a pivotal role in ascorbate biosynthesis. Recent studies have proposed that the biosynthetic enzymes in the cytosol form a protein complex (Fenech *et al.*, 2021), potentially contributing to the regulation of ascorbate biosynthesis. Additionally, ascorbate itself tightly regulates its biosynthesis. High ascorbate levels repress VTC2 translation via an upstream open reading frame (uORF) in the 5′-untranslated region of the gene, counterbalancing the light-induced activation of GGP (Laing *et al.*, 2015). Consequently, ascorbate biosynthesis is finely tuned through transcriptional, translational, and post-translational regulation. However, the precise mechanisms underlying light-dependent GGP activation remain to be elucidated.

The *VTC3* gene encodes a unique protein with both serine/threonine kinase and PP2C domains (Conklin *et al.*, 2000, 2013). Two distinct *vtc3* alleles have been identified: *vtc3-1*, which carries a G202E missense mutation in the kinase domain, and *vtc3-2*, which has a nonsense mutation

in the PP2C domain (Conklin *et al.*, 2013). Both alleles exhibit a moderate ascorbate-deficient phenotype, with approximately 50% of wild-type ascorbate levels, a deficiency less severe than that observed in *vtc2* mutants (20–30% of wild-type levels). VTC3 is highly conserved across land plants and algae (Conklin *et al.*, 2013; Maruta *et al.*, 2024), and its loss also results in ascorbate deficiency in the moss *Physcomitrella patens* (Sodeyama *et al*., 2021). Notably, light-induced ascorbate accumulation is significantly impaired in Arabidopsis *vtc3* mutants (Conklin *et al.*, 2013), suggesting that VTC3 plays a crucial role in the light regulation of VTC2/GGP. Since VTC3 has been reported to be a chloroplast protein, it is unlikely to regulate ascorbate biosynthesis through direct (de)phosphorylation of biosynthetic enzymes. The precise physiological function of VTC3 remains unclear, and further studies are required to elucidate its role.

The size of the ascorbate pool is regulated not only by biosynthesis but also by its oxidation, recycling, and degradation. Reduced ascorbate (ASC) undergoes oxidation through APX or direct interaction with ROS, generating monodehydroascorbate (MDHA) (Asada, 1999; Smirnoff, 2018). MDHA radicals are disproportionated into ASC and dehydroascorbate (DHA). MDHA and DHA are recycled back to ASC by monodehydroascorbate reductase (MDAR) and dehydroascorbate reductase (DHAR), respectively (Foyer and Halliwell, 1977; Hossain and Asada, 1985). MDAR uses NAD(P)H, while DHAR relies on reduced glutathione (GSH) as the electron donor. Additionally, GSH can nonenzymatically reduce DHA to ASC (Winkler *et al.*, 1994; Terai *et al.*, 2020; Hamada *et al.*, 2023). However, DHA is highly unstable and undergoes irreversible degradation if not rapidly reduced. These interconnected processes are essential for maintaining ascorbate homeostasis. These interconnected processes are essential for maintaining ascorbate homeostasis, and it remains possible that VTC3 regulates ascorbate pool size by modulating ascorbate oxidation or degradation processes.

This study addresses two unresolved questions regarding the regulation of ascorbate homeostasis in plants. First, although VTC2/GGP is known to be a key regulatory enzyme in ascorbate biosynthesis and is strongly induced by light, the upstream signaling components controlling its activation remain poorly understood. Previous studies reported that *vtc3* mutants exhibit defective light-induced ascorbate accumulation (Conklin *et al*., 2013), suggesting a possible regulatory link between VTC3 and VTC2/GGP expression or activity. Based on this, we hypothesized that VTC3 facilitates the light-dependent activation of VTC2/GGP and thereby promotes ascorbate biosynthesis under light stress. Second, while *vtc2* and *vtc3* single mutants both show ascorbate deficiency, their distinct phenotypes raise the question of whether these genes act independently or synergistically. Notably, *vtc2* mutants retain the ability to increase ascorbate levels under high-light stress, likely due to the residual function of the minor GGP isoform VTC5 (Hamada *et al*., 2023; Terai *et al*., 2020),

150 whereas *vtc3* mutants fail to induce this response (Conklin *et al*., 2013). We therefore hypothesized
151 that the simultaneous loss of both genes would result in a more severe ascorbate-deficient phenotype
152 and increased light stress sensitivity. By characterizing single and double mutants of *vtc2* and *vtc3*, we
153 aimed to test these hypotheses and gain new insights into the genetic and physiological control of
154 ascorbate metabolism and photoprotection in Arabidopsis.
155
156 **Materials and methods**
157 **Plant Materials and Growth Conditions**
158 *Arabidopsis thaliana* ecotype Col-0 was used as the wild type. The T-DNA insertion lines *vtc2-4*
159 (SAIL_769_H05) and *vtc3-3* (SALK_095743) were obtained from the Arabidopsis Biological
160 Resource Center and used for further crossings. Unless otherwise specified, wild-type and mutant
161 seeds were sown in Jiffy-7 peat pellets and stratified in the dark at 4°C for 2–3 days. Plants were grown
162 in a growth chamber (KCLP-1000CCFL-6-8L-CO_2, NK System) at 22°C under a 16-hour photoperiod
163 with low light intensity (40–60 µmol photons m^{-2} s^{-1}) and at 20°C in darkness for 8 hours. At three
164 weeks of age, plants were exposed to moderate- or high-light stress (750 or 1,500 µmol photons m^{-2}
165 s^{-1}) using an LED lighting unit (PFQ-600PT, NK System) without a preceding dark period. The LED
166 system minimized heat production, maintaining leaf temperature at approximately 24–25°C. To ensure
167 uniform light exposure, plants were placed on a turntable beneath the LED panel. Fully expanded
168 rosette leaves were collected from at least three plants and treated as a single biological replicate.
169 Rosette and lesion areas (percentage of the total rosette area) were quantified using ImageJ software.
170 For ascorbate complementation assays, fully expanded leaves were excised from 3-week-
171 old plants and floated on 20 mM MES buffer (pH 5.7), with or without 10 mM sodium ascorbate. The
172 samples were incubated under continuous light for 24 h, followed by exposure to high-light conditions
173 for an additional 24 h. Thereafter, leaves were subjected to trypan blue staining to visualize cell death.
174 The stained area was quantified using ImageJ software.
175 For plate-grown experiments (**Figures 3 and 4**), wild-type and mutant plants were
176 cultivated on half-strength Murashige and Skoog (MS) medium supplemented with 1% sucrose under
177 a 16-hour photoperiod at 100 µmol photons m^{-2} s^{-1} and 22°C, with an 8-hour dark period at 20°C (LH-
178 240S, NK System). Plants were then subjected to moderate-light stress (650 µmol photons m^{-2} s^{-1})
179 without an intermediate dark period using the same LED panel and turntable system. Shoots from at
180 least ten plants were pooled and treated as a single biological replicate.
181
182 **Semi-quantitative and quantitative reverse transcription-polymerase chain reaction**

183 Semi-quantitative reverse transcription-polymerase chain reaction (RT-PCR) was performed
184 according to Terai *et al*. (2020). Quantitative RT-PCR (qPCR) was performed as described by Iwagami
185 *et al*. (2022). *Actin2* mRNA was used as an internal standard in all experiments. The expression
186 stability of *Actin2* was confirmed by evaluating C*t* values across all experimental conditions. Three
187 biological replicates per genotype/treatment combination were used, and each was derived from the
188 average of three technical qPCR replicates. Expression variability was assessed using the coefficient
189 of variation (CV). The consistently low CV values (ranging from 0.4% to 1.32%) support the use of
190 *Actin2* as a stable reference gene under the tested conditions (see **Supplementary Figure S1**). All the
191 primers used are listed in **Supplementary Table S1**.
192
193 **Western blotting**
194 To examine VTC2 protein expression, we attempted to generate two independent anti-VTC2 peptide
195 antibodies. The peptide sequences used were "NH_2-C+QNSSGNVNQKSNRT-COOH" and "NH_2-
196 C+KRKEDYEGASEDNA-COOH". The design and synthesis of the antigenic peptides, as well as
197 antibody production, were outsourced to Eurofins Genomics. In addition, we purchased a commercial
198 anti-GDP-L-galactose phosphorylase antibody (AS10 723, Agrisera). Using these antibodies, we
199 performed western blotting following the method described by Kameoka *et al*. (2021), but we were
200 unable to detect the VTC2 protein.
201
202 **Measurements of Antioxidants and Enzyme Activity**
203 Ascorbate content was quantified using an ultra-fast liquid chromatography (UFLC) system equipped
204 with a C18 column, following the method of Hamada and Maruta (2024). Glutathione levels were
205 measured according to Noctor *et al.* (2016) without modifications. Soluble and membrane-bound APX
206 activity was assessed using the method described by Kameoka *et al.* (2021), while DHAR and MDAR
207 activities were measured as outlined by Tanaka *et al.* (2021).
208 GGP activity was measured according to Hamada *et al*., (2023). *Arabidopsis* leaves (0.2
209 g) frozen in liquid nitrogen were ground and homogenized in 1 mL of extraction buffer containing 50
210 mM Tris–HCl (pH 7.5), 10% glycerol, 2 mM DTT, 10 mM $MgCl_2$, 1 mM aminocaproic acid, 1 mM
211 benzamidine, 1 mM phenylmethanesulfonylfluoride. After centrifugation (15,300 × *g*) for 20 min at
212 4 °C, the supernatant was concentrated by ultrafiltration (15,300 × *g*, 30 min, 4 °C) using an Amicon
213 ultra centrifugal filter (10 kDa, NMWL) and used for the following assay. The extract (20 µL) was
214 added to 80 µL of a reaction mixture containing 50 mM Tris–HCl (pH 7.5), 2 mM $MgCl_2$, 10 mM
215 KCl, 1mM dithiothreitol, and 100 µM GDP-D-glucose with or without 5 mM sodium phosphate and

incubated for 1 h at 26 °C. The reaction was stopped by boiling for 5 min, and the mixture was passed through 0.22 µm filters (Merck Millipore). The samples were injected into an ultra-fast liquid chromatography (UFLC) system (Prominence UFLC, Shimadzu) equipped with a C-18 column (LUNA C18(2), Column 150 x 4.6 nm, Shimadzu). The mobile phase consisted of 50 mM phosphate buffer (pH 6.7), 5 mM tetrabutylammonium dihydrogen phosphate, 5 mg L^{-1} EDTA, and 3.5% methanol, and the flow rate was 1 mL min^{-1}. GDP-D-glucose was detected at 254 nm using the SPD-20A UV-Vis detector (Shimadzu). Pi-independent degradation was subtracted from the Pi-dependent decrease in the substrate to calculate GDP-D-glucose degradation activity.

RNA-Seq Analysis

Two-week-old wild-type, *vtc2-4*, and *vtc3-3* seedlings, grown on half-strength MS medium supplemented with 1% sucrose under the same conditions described above, were incubated in darkness for two days, followed by a six-hour exposure to growth light (100 µmol photons m^{-2} s^{-1}). Total RNA was extracted from shoot tissues using RNAiso Plus (Takara, Japan) and purified with NucleoSpin RNA Plus (Takara). RNA was fragmented and converted to double-stranded DNA using the TruSeq RNA Sample Preparation Kit v2 (Illumina). Library quality and quantity were assessed using a Bioanalyzer (Agilent) and a KAPA Library Quantification Kit (KAPA Biosystems), respectively. Sequencing was performed using an Illumina MiSeq with the MiSeq Reagent Kit v3 (300 cycles; Illumina). RNA-seq data were obtained from triplicate biological samples (n = 3 per group) and statistically analyzed. Read mapping, data processing, and statistical analyses were conducted using the CLC Genomics Workbench (version 9.5.2). The gene expression dataset has been deposited in the Gene Expression Omnibus under accession number GSE293768. Gene ontology (GO) enrichment analysis was performed using agriGO (version 2; Tian *et al.*, 2017).

Chlorophyll Fluorescence Measurements

Chlorophyll fluorescence measurements were performed using a Closed FluorCam 800MF (Photon Systems Instruments). Plants were dark-adapted for 30 minutes before measurements. Chlorophyll fluorescence parameters, F_v/F_m and NPQ, were calculated according to Baker (2008) using the following equations: $F_v/F_m = (F_m - F_o)/F_m$, and $NPQ = (F_m - F_m')/F_m'$. NPQ was measured under actinic light at an intensity of 90 µmol photons m^{-2} s^{-1}.

Accession Numbers

VTC2, At4g26850; VTC3, At2g40860.

249

250 **Data Analysis**

251 The statistical methods used are described in the respective figure legends (Tukey–Kramer, Dunnett's
252 test, or Student's *t*-test). Statistical calculations were performed using at least three independent
253 biological replicates (see figure legends for details).

254

255 **Results**

256 ***VTC3 is required for ascorbate accumulation under high-light stress***

257 To evaluate the role of VTC3 in ascorbate accumulation under high-light conditions, we used a T-
258 DNA insertion mutant for the *VTC3* gene, referred to hereafter as *vtc3-3* (Conklin *et al*., 2013), as well
259 as the *vtc2-4* mutant (Lim *et al*., 2016). In *vtc3-3*, the T-DNA is inserted in the seventh exon of *VTC3*,
260 whereas in *vtc2-4*, the insertion occurs in the third exon of *VTC2*. Both mutants have been previously
261 characterized as null alleles, lacking full-length transcripts of the respective genes (Conklin *et al*.,
262 2013; Lim *et al*., 2016). This was further confirmed by our RT-PCR analysis (**Supplementary Figure**
263 **S2**). Under low-light conditions, *vtc2-4* and *vtc3-3* mutants exhibited approximately 26% and 45% of
264 wild-type ascorbate levels, respectively (**Figure 1A**), consistent with previous reports (Conklin *et al.*,
265 2013; Lim *et al.*, 2016). Exposure to high-light stress induced a time-dependent increase in ascorbate
266 content in wild-type plants. In contrast, the *vtc3-3* mutant displayed only a minimal and statistically
267 insignificant increase in ascorbate levels. The ascorbate pool size in *vtc2-4* remained significantly
268 lower than in wild-type plants under both low-light and high-light conditions. However, high-light
269 stress markedly increased ascorbate levels in *vtc2-4* (**Figure 1A**), corroborating previous findings
270 (Hamada *et al*., 2023; Terai *et al*., 2020). The elevated amounts of ascorbate after 48 hours of high-
271 light exposure were approximately 5.5 μmol g^{-1} FW in the wild type, 3.4 μmol g^{-1} FW in *vtc2-4*, and
272 0.7 μmol g^{-1} FW in *vtc3-3* (**Figure 1B**). Neither the *vtc2-4* nor *vtc3-3* mutation affected the ascorbate
273 redox state under either low- or high-light conditions. These results demonstrate that VTC3 is essential
274 for the accumulation of ascorbate in response to high-light exposure.

275

276 ***VTC3 is not required for VTC2 expression or GGP enzyme activity***

277 To test our first hypothesis that VTC3 regulates the light-dependent activation of VTC2/GGP, we
278 analyzed the transcript levels of *VTC2* and *VTC5* before and after 24 hours of high-light exposure. In
279 *vtc2-4* mutants, *VTC2* transcripts were nearly undetectable (**Figure 1C**). In wild-type plants, the
280 transcript levels of both *VTC2* and *VTC5* showed a modest increase in response to high-light stress.
281 Intriguingly, these increases were more pronounced in *vtc3-3* mutants. This upregulation of *VTC2* and

282 *VTC5* in *vtc3-3* mutants may represent a compensatory response to ascorbate deficiency. However, no
283 similar increase in *VTC5* expression was observed in *vtc2-4* mutants after high-light exposure (**Figure**
284 **1D**), possibly because *vtc2-4* mutants retained higher ascorbate levels than *vtc3-3* mutants under high-
285 light conditions (**Figure 1A**).
286 To assess VTC2 protein levels, we obtained three anti-VTC2 antibodies targeting different
287 VTC2 peptides. Unfortunately, none of these antibodies successfully detected VTC2 via western
288 blotting, likely due to low antibody specificity or the very low abundance of VTC2 protein. As an
289 alternative, we measured GGP activity using a Pi-dependent GDP-D-glucose degradation assay, a
290 reliable indicator of endogenous GGP activity (Hamada *et al*., 2023). In wild-type plants, GGP activity
291 increased in response to high-light exposure, whereas in *vtc2-4* mutants, activity was nearly
292 undetectable (**Figure 1E**). Notably, the absence of VTC3 did not reduce GGP activity; rather, it
293 appeared to enhance it, consistent with the observed increase in *VTC2* and *VTC5* transcript levels in
294 *vtc3-3* mutants. Contrary to our hypothesis, these results indicate that VTC3 is not essential for the
295 expression and activity of GGP.
296
297 ***VTC3 does not affect ascorbate redox enzyme activities or transcriptome profiles***
298 We next speculated that VTC3 may contribute to ascorbate redox cycling rather than biosynthesis. To
299 test this possibility, we examined the impact of VTC3 on glutathione levels and the activities of APX,
300 DHAR, and MDAR. Plants grown under plate conditions were used for these experiments. Two-week-
301 old wild-type, *vtc2-4*, and *vtc3-3* plants on agar plates were exposed to moderate-light stress (650
302 μmol photons m^{-2} s^{-1}; ML^{650}) for 24 hours. This stress increased ascorbate levels in both wild-type and
303 *vtc2-4* plants, but this response was nearly absent in *vtc3-3* mutants, consistent with the data obtained
304 from *in vivo* soil experiments (**Figure 2**).
305 The size of the glutathione pool increased under ML^{650} stress in all genotypes, with no
306 significant differences observed among the wild type, *vtc2-4*, and *vtc3-3*. Additionally, APX, DHAR,
307 and MDAR activities were upregulated under these conditions, but neither *vtc2-4* nor *vtc3-3* mutations
308 influenced their activities under either low-light or stress conditions (**Figure 2**). These findings suggest
309 that VTC3 does not significantly affect ascorbate redox cycling.
310 To further investigate the function of VTC3, we performed transcriptome analysis. For this
311 experiment, a drastic light/dark shift was used instead of light stress to induce a stronger response.
312 Two-week-old wild-type, *vtc2-4*, and *vtc3-3* plants grown on agar plates under low-light conditions
313 were incubated in darkness for two days, followed by a 6-hour exposure to growth light (100 μmol
314 photons m^{-2} s^{-1}). Differentially expressed genes (false discovery rate < 0.05) were identified from

315 triplicate datasets by comparing the mutants to wild-type plants (**Figure 3**). In total, over 200 genes
316 were differentially expressed in *vtc2-4* mutants, whereas only 24 genes, including *VTC3* itself, were
317 affected in *vtc3-3* mutants. Among these, seven genes were commonly affected in both mutants. The
318 relatively minor transcriptomic impact of VTC3 compared to VTC2 likely reflects the weaker
319 ascorbate-deficient phenotype of *vtc3-3*. Gene ontology (GO) enrichment analysis showed that
320 "defense response to pathogens" was the most enriched GO term among the 12 genes upregulated in
321 *vtc3* mutants (**Figure 3**). Furthermore, downregulated genes specific to *vtc3-3* included cytochrome
322 P450 superfamily protein (AT3G44970), transmembrane protein (AT5G01881), mto1 responding
323 down 1 (AT1G53480), and phosphoinositide 4-kinase gamma 1 (AT2G40850), none of which are
324 known to be directly associated with ascorbate metabolism. These results suggest that VTC3 plays a
325 more limited role in transcriptomic regulation than VTC2.
326
327 ***Simultaneous loss of VTC2 and VTC3 exacerbates ascorbate deficiency and increases light stress***
328 ***sensitivity***
329 To test our second hypothesis that the simultaneous loss of VTC2 and VTC3 would result in additive
330 or synergistic effects on ascorbate pool size, we generated and analyzed *vtc2-4 vtc3-3* double mutants
331 under both low- and high-light conditions. Homozygous double mutants were identified by genotyping
332 the F_2 population following crossing (**Supplementary Figure S2**). Compared to single mutants, the
333 double mutants exhibited the lowest ascorbate levels, retaining only approximately 51% of the
334 ascorbate content observed in *vtc2-4* single mutants, equivalent to about 14% of wild-type levels
335 (**Figure 4**). Notably, except for mutants entirely lacking detectable ascorbate (e.g., *vtc2 vtc5* double
336 mutants), *vtc2-4 vtc3-3* double mutants displayed the lowest ascorbate levels reported among
337 ascorbate-deficient mutants. Despite these extremely low levels, their growth under low-light
338 conditions for three weeks was comparable to that of wild-type plants and single mutants (**Figure 4**),
339 suggesting that even 14% of wild-type ascorbate levels is sufficient to support Arabidopsis growth
340 under controlled laboratory conditions.
341 When exposed to high-light stress for 24 hours, *vtc2-4* and *vtc3-3* single mutants exhibited
342 photo-bleaching, primarily in older leaves (**Figure 5**). In contrast, the *vtc2-4 vtc3-3* double mutants
343 displayed a more severe photo-bleaching phenotype, extending to mature leaves, and exhibited the
344 most pronounced cell death, consistent with their extremely low ascorbate content. Reflecting these
345 phenotypes, the reduction in the maximum quantum yield of photosystem II (F_v/F_m) under high-light
346 stress was most pronounced in the double mutants (**Figure 5**), indicating severe damage to
347 photosynthesis. To test whether the heightened light sensitivity of the double mutants is attributable to

348 ascorbate deficiency, we conducted a chemical complementation experiment using sodium ascorbate.
349 Detached leaves from 3-week-old *vtc2-4 vtc3-3* plants were floated on buffer with or without 10 mM
350 sodium ascorbate under continuous light for 24 h, followed by 24 h of high-light exposure. Under
351 these conditions, clear leaf bleaching and intense trypan blue staining were observed only in *vtc2-4*
352 *vtc3-3* leaves without sodium ascorbate treatment. Notably, these symptoms were completely
353 abolished by sodium ascorbate treatment (**Supplementary Figure S3**), indicating that the severe
354 photooxidative damage in the double mutants is primarily due to their profound ascorbate deficiency.
355 Considering the heightened sensitivity of *vtc2-4 vtc3-3* mutants to high-light stress, we
356 measured ascorbate content in wild-type plants and mutants during the early stages of high-light
357 exposure (6 and 12 hours). Ascorbate levels in wild-type plants and *vtc2-4* mutants increased
358 approximately 1.5-fold by 12 hours after high-light exposure (**Figure 6**), but there was no statistical
359 difference. Furthermore, no significant increase in ascorbate levels was observed in *vtc3-3* or *vtc2-4*
360 *vtc3-3* mutants. However, the early-stage ascorbate increase in wild-type plants and *vtc2-4* mutants
361 was relatively modest (**Figure 6**), making detailed comparisons between mutants challenging.
362 To further investigate the ascorbate accumulation response under different light intensities,
363 we conducted similar experiments under moderate-light conditions (750 µmol photons m^{-2} s^{-1}; ML^{750}).
364 Under ML^{750} stress, ascorbate accumulation was observed even in *vtc3-3* and *vtc2-4 vtc3-3* mutants;
365 however, the increase was significantly smaller compared to *vtc2-4*, with the double mutants
366 exhibiting the lowest levels of stress-induced ascorbate accumulation (**Figure 6**). These results
367 demonstrate that the simultaneous knockout of VTC2 and VTC3 severely limits both steady-state
368 ascorbate levels and stress-induced ascorbate accumulation, thereby dramatically increasing
369 sensitivity to photooxidative stress.
370
371 ***Impaired induction of non-photochemical quenching in* vtc2-4 vtc3-3 *double mutants***
372 As ascorbate is implicated in the induction of NPQ (Müller-Moulé *et al.*, 2004), a photoprotective
373 mechanism that dissipates excess absorbed light energy as heat, we investigated how the severe
374 ascorbate deficiency in *vtc2-4 vtc3-3* double mutants affects NPQ. Plants were grown under low-light
375 conditions for three weeks before being subjected to high-light stress for 24 hours. Under low-light
376 conditions, NPQ induction was partially suppressed in all mutants compared to wild-type plants, with
377 statistically significant but relatively small differences (**Figure 7A and C**). Among the single mutants,
378 *vtc2-4* exhibited a greater reduction in NPQ induction compared to *vtc3-3*, consistent with its lower
379 ascorbate pool size. Although the *vtc2-4 vtc3-3* double mutants showed a trend toward further reduced
380 NPQ values, the difference was not statistically significant compared to *vtc2-4* single mutants.

381 Following high-light exposure, NPQ suppression was most pronounced in *vtc2-4 vtc3-3* double
382 mutants, significantly lower than in either *vtc2-4* or *vtc3-3* single mutants (**Figure 7B and D**).
383 Interestingly, while *vtc2-4* exhibited lower NPQ values than *vtc3-3* under low-light conditions (**Figure**
384 **7C**), this difference disappeared under high-light stress. (**Figure 7D**) These variations in NPQ
385 induction closely paralleled the differences in ascorbate pool sizes among the mutants. These findings
386 provide new insights into the relationship between NPQ induction and ascorbate levels, highlighting
387 the additive effects of *vtc2-4* and *vtc3-3* mutations on NPQ suppression under high-light stress. The
388 results suggest that ascorbate plays a critical role in NPQ induction under both low- and high-light
389 conditions and that VTC2 and VTC3 contribute to this regulation through their roles in ascorbate
390 accumulation.
391
392 **Discussion**
393 Among the *vtc* mutant series, *vtc3* is the only mutant with a mutation in a gene that does not encode a
394 biosynthetic enzyme (Conklin *et al*., 2013). VTC3 is a unique protein containing both protein kinase
395 and phosphatase domains and is essential for ascorbate accumulation in response to continuous
396 exposure to growth light. Given that VTC2/GGP is the rate-limiting enzyme in ascorbate biosynthesis
397 and that its expression and activity are enhanced by light, we initially hypothesized that VTC3
398 regulates ascorbate biosynthesis at the VTC2/GGP step. However, this hypothesis was strongly refuted,
399 as the loss of VTC3 did not reduce *VTC2/VTC5* transcription or GGP activity (**Figure 1**). As
400 previously reported, VTC2 translation is controlled by ascorbate via an uORF in the 5′-untranslated
401 region of the *VTC2* gene (Laing *et al*., 2015). Because we were unable to examine VTC2/GGP
402 expression at the protein level, we cannot entirely rule out the possibility that VTC3 influences VTC2
403 translation. However, if this were the case, the absence of VTC3 would likely lead to reduced GGP
404 activity, which was not observed (**Figure 1**). Thus, we conclude that VTC3 is not required for the
405 expression and activity of VTC2/GGP.
406 We also found that the loss of VTC3 did not affect glutathione profiles or the activities of
407 APX, DHAR, and MDAR (**Figure 2**). Since we did not examine the expression or activity of
408 individual isoforms of these enzymes, we cannot rule out the possibility that VTC3 affects ascorbate
409 redox cycling in specific compartments. However, recent studies have demonstrated that the
410 complementary actions of MDARs, DHARs, and glutathione maintain a robust ascorbate recycling
411 system in Arabidopsis (Maruta *et al.,* 2024). For instance, the loss of all three *DHAR* genes has a
412 negligible impact on ascorbate levels, even under stress conditions (Rahantaniaina *et al.*, 2017; Terai
413 *et al.*, 2020). Considering the resilience of the ascorbate recycling system, it is unlikely that VTC3

414 plays a role in regulating ascorbate redox cycling. Another possible function of VTC3 could be the
415 inhibition of ascorbate degradation. However, this is also unlikely, as ascorbate degradation begins
416 with DHA, and ascorbate recycling capacity was unaffected in *vtc3* mutants.

417 Since VTC3 contains both protein kinase and phosphatase domains, it was also plausible
418 that it mediates light-dependent signaling pathways to enhance ascorbate pool size. However,
419 transcriptome analysis revealed that only a limited number of genes were specifically up- or
420 downregulated in *vtc3-3* mutants (**Figure 3**), and none had known associations with ascorbate
421 metabolism. However, one of the genes downregulated in *vtc3-3* mutants encodes phosphoinositide 4-
422 kinase gamma 1 (PI4Kγ1). Although this gene has not been directly linked to ascorbate metabolism,
423 it may affect the pool size of *myo*-inositol, a potential precursor of ascorbate in the alternative
424 biosynthetic pathway (Lorence et al., 2004). While the physiological relevance of this pathway in
425 Arabidopsis remains under debate (Maruta, 2022), the potential role of PI4Kγ1 in regulating ascorbate
426 levels through myo-inositol metabolism warrants further investigation. GO enrichment analysis
427 identified "defense response to pathogens" as the most enriched term among the 12 genes whose
428 expression was specifically enhanced in *vtc3* mutants (**Figure 3 and Supplementary Table S2**). This
429 finding aligns with previous observations in *vtc1* mutants, where ascorbate deficiency was linked to
430 enhanced pathogen responses (Pastori *et al.*, 2003). Thus, the transcriptional activation of some
431 defense-related genes in *vtc3-3* mutants is likely a secondary effect of ascorbate deficiency rather than
432 the direct involvement of VTC3 in defense signaling. In *vtc2-4* mutants, 115 genes were upregulated
433 (**Figure 3**), with GO terms related to "response to salicylic acid" and "response to chitin" enriched
434 (**Supplementary Table S2**), further suggesting a link between ascorbate deficiency and pathogen
435 responses.

436 In our RNA-seq analysis, we identified 210 differentially expressed genes (DEGs) in the
437 *vtc2-4* mutant (**Figure 3**). This number is substantially lower than the 963 DEGs previously reported
438 in *vtc2* mutants by Kerchev *et al*. (2011), who used microarray analysis. This discrepancy is likely due
439 to differences in experimental conditions. In our study, 2-week-old seedlings were grown aseptically
440 on agar plates under long-day conditions, followed by 48 hours of darkness and a 6-hour light
441 treatment before sampling. In contrast, Kerchev *et al*. (2011) used fully mature 6-week-old plants
442 grown in soil under short-day conditions. These differences in plant age, growth medium, and light
443 regime likely contributed to the differing transcriptome responses. Moreover, only 11 out of the 119
444 upregulated genes in *vtc2-4* overlapped with the 378 upregulated genes in the *vtc2* dataset from
445 Kerchev *et al*. (2011) (**Supplementary Table S2**), suggesting the condition-specific nature of
446 transcriptomic responses to ascorbate deficiency. However, both studies consistently observed an

447 increase in the expression of pathogen-response-related genes, suggesting this may be a core feature
448 of ascorbate deficiency. Since the transcriptomic consequences of ascorbate deficiency remain
449 incompletely understood, further comparative studies under standardized conditions will be important
450 to clarify its context-dependent effects.

451 Taken together, these findings indicate that the loss of VTC3 has minimal impact on
452 VTC2/GGP, ascorbate redox cycling, or the transcriptome. Nevertheless, the impaired light-induced
453 ascorbate accumulation observed in *vtc3-3* mutants suggests that VTC3 may regulate ascorbate
454 biosynthesis at steps other than VTC2/GGP. One plausible possibility is that VTC3 influences
455 enzymes upstream of VTC2 in the D-Man/L-Gal pathway, such as PMI, PMM, GMP, and GME. These
456 enzymes are responsible for synthesizing GDP-L-galactose, the direct substrate of VTC2/GGP, and
457 reduced activity in any of these steps could limit VTC2 function despite unaltered transcript levels and
458 enzyme activity. Alternatively, VTC3 may affect the supply of essential cofactors required for the
459 optimal activity of VTC2/GGP or its upstream enzymes. For example, VTC2/GGP activity is
460 dependent on the availability of inorganic phosphate. Further studies will be required to identify the
461 precise molecular targets of VTC3 and to clarify how it contributes to the light-responsive regulation
462 of ascorbate biosynthesis. Given that *VTC3* encodes a putative kinase/phosphatase, it may also play
463 broader regulatory roles beyond ascorbate biosynthesis.

464 Consistent with previous reports (Terai *et al.*, 2020; Hamada *et al.*, 2023), *vtc2-4* mutants
465 retained the ability to increase ascorbate accumulation in response to light stress (**Figure 1**). We
466 initially hypothesized that this ability might be due to the activation of residual VTC5. However, *VTC5*
467 transcription showed little to no increase in *vtc2-4* mutants compared to the wild type, and GGP
468 activity was nearly undetectable in *vtc2-4* mutants even under high-light stress (**Figure 2**). This could
469 be due to GGP activity in *vtc2-4* being below the detection limit. Indeed, the simultaneous loss of
470 VTC2 and VTC5 results in ascorbate levels below the detection limit, indicating that VTC5 functions
471 as an active enzyme in ascorbate biosynthesis (Dowdle *et al.*, 2007; Lim *et al.*, 2016). Alternatively,
472 because we used GDP-D-glucose instead of GDP-L-galactose (the physiological substrate, which is
473 commercially unavailable) to measure GGP activity, our assay may not fully reflect endogenous GGP
474 activity. Nevertheless, it is intriguing that ascorbate levels in *vtc2* mutants can increase significantly
475 without a measurable increase in GGP activity. If alternative biosynthetic pathways are not considered,
476 this suggests a mechanism that enhances the GGP response independent of measurable GGP activity.
477 The recently reported metabolon formation of ascorbate biosynthetic enzymes may be involved
478 (Fenech *et al.*, 2021), but further experimental validation is required.

479 Another key objective of this study was to examine the impact of the simultaneous loss of

480 VTC2 and VTC3 on ascorbate pool size. As expected, *vtc2-4 vtc3-3* double mutants exhibited the
481 lowest ascorbate levels reported among viable ascorbate-deficient mutants, retaining only about 14%
482 of wild-type levels (**Figure 4**). Nevertheless, under low-light conditions, *vtc2-4 vtc3-3* double mutants
483 displayed a healthy phenotype similar to wild-type plants. The original *vtc2-1* mutant, isolated via an
484 ethyl methanesulfonate (EMS) mutagenesis screen, has been reported to exhibit dwarfism under
485 standard growth conditions, whereas the T-DNA insertion mutant *vtc2-4*, despite having comparable
486 ascorbate levels, does not exhibit dwarfism (Lim *et al*., 2016). It has been suggested that the dwarfism
487 observed in *vtc2-1* may be due to a mutation in another gene. The relationship between ascorbate
488 levels and growth must be carefully evaluated, as it is highly influenced by growth light intensity. For
489 instance, when grown under relatively higher light conditions (200 µmol photons m^{-2} s^{-1}), both *vtc2-1*
490 and *vtc2-4* exhibit similar degrees of dwarfism (Plumb *et al.*, 2018). Considering this complexity, our
491 data suggest that under artificial low-light conditions, as little as 14% of wild-type ascorbate levels
492 are sufficient for normal growth in Arabidopsis. This finding provides the idea that the primary reason
493 plants accumulate high concentrations of ascorbate is to protect against oxidative stress rather than to
494 fulfill its coenzyme functions.

495 The loss of VTC3 significantly impaired high-light-induced ascorbate accumulation in
496 both wild-type and *vtc2-4* backgrounds (**Figure 6**). *vtc2-4 vtc3-3* double mutants maintained
497 extremely low ascorbate levels even under high-light conditions, leading to more severe
498 photooxidative damage than either single mutant (**Figure 5**). In terms of photobleaching severity, *vtc2-*
499 *4* was more sensitive to high light than *vtc3-3*, and the sensitivity of the double mutant was entirely
500 consistent with its steady-state ascorbate pool size (**Figure 5**). NPQ values were statistically
501 significantly lower in all *vtc* mutants compared to wild-type plants under low-light conditions, with
502 *vtc2-4* and the double mutant exhibiting greater reductions than *vtc3-3* (**Figure 7**). However, no
503 significant difference was observed between *vtc2-4* and the double mutant under low-light conditions,
504 suggesting that NPQ suppression due to ascorbate deficiency may reach a threshold at ~30% of wild-
505 type ascorbate levels. Interestingly, this difference became more pronounced after high-light exposure,
506 paralleling the fact that *vtc2-4* mutants still exhibited light-induced ascorbate accumulation, whereas
507 this response was severely impaired in the double mutants (**Figure 6**). So far, *vtc1* and *vtc4* mutants
508 have also been used to study ascorbate deficiency, but these mutants have pleiotropic effects unrelated
509 to ascorbate metabolism (Torabinejad *et al.*, 2009; Barth *et al.*, 2010). In contrast, *vtc2-4* and *vtc3-3*
510 mutants provide a more targeted approach. Since the *vtc2-4 vtc3-3* double mutant retains the
511 characteristics of both single mutants, comparative analysis of these mutants represents a powerful
512 tool for elucidating the physiological roles of ascorbate.

513 In conclusion, our findings indicate that VTC3 is not required for the expression or activity
514 of VTC2/GGP, ascorbate redox cycling (including ascorbate recycling), or the regulation of the
515 transcriptome. These negative results provide important insight by excluding several plausible roles
516 of VTC3 and thereby advancing our understanding of its physiological function. While the
517 fundamental function of VTC3 remains unresolved, our findings suggest that VTC3 regulates
518 ascorbate biosynthesis at a step other than VTC2/GGP, and future research will focus on validating
519 this notion. Furthermore, this study revealed that the simultaneous knockout of VTC2 and VTC3
520 exacerbates ascorbate deficiency and increases sensitivity to light stress, likely due to the combined
521 loss of ascorbate biosynthesis capacity (via VTC2) and regulatory modulation (via VTC3), both of
522 which are essential for maintaining sufficient ascorbate levels under photooxidative stress. The newly
523 generated *vtc2-4 vtc3-3* double mutant retains only 14% of wild-type ascorbate levels. Given its
524 distinct physiological characteristics, such as impaired non-photochemical quenching and enhanced
525 photooxidative stress sensitivity, this double mutant, in combination with the single mutants, provides
526 a valuable genetic tool to further dissect the relationship between ascorbate levels and physiological
527 responses. Notably, it represents the most severely ascorbate-deficient viable Arabidopsis mutant
528 characterized to date, potentially enabling the discovery of previously unrecognized roles of ascorbate
529 in plant physiology.
530
531 **Figure legends**
532 **Figure 1** Ascorbate accumulation and GGP expression/activity in *vtc3-3* under high light
533 Wild-type, *vtc2-4*, and *vtc3-3* plants were grown in soil under low-light (40–60 μmol photons m^{-2} s^{-1})
534 conditions for three weeks and then exposed to high-light stress (1,500 μmol photons m^{-2} s^{-1}) for 48
535 h. Fully expanded leaves were used in subsequent experiments. (A) Total ascorbate content (sum of
536 ASC and DHA contents). (B) The amounts of ascorbate increase from before to after high-light
537 exposure (48 h). (A, B) Data are presented as the mean ± SE of four biological replicates. Different
538 letters indicate significant differences ($P < 0.05$, one- or two-way ANOVA followed by Tukey–Kramer
539 test). (C, D) Transcript levels of *VTC2* and *VTC5* were determined using qPCR analysis. (E) GGP
540 activity was determined as GDP-D-glucose degrading activity. Data are presented as the mean ± SE
541 of three biological replicates. (C, E) Significant differences between wild type and *vtc3-3* (Student's
542 *t*-test): $^{*}P < 0.05$, $^{**}P < 0.01$, versus the values of the wild-type plants. Because *VTC2* transcript levels
543 and GGP activity were negligible in *vtc2-4*, statistical analysis was performed only between wild-type
544 and *vtc3-3*. (B) Different letters indicate significant differences between genotypes ($P < 0.05$, one-way
545 ANOVA followed by Tukey–Kramer test). ASC, reduced ascorbate; DHA, dehydroascorbate; FW,

546 fresh weight.
547
548 **Figure 2** Antioxidant levels and enzyme activities related to ascorbate redox turnover in *vtc3-3* under
549 high light
550 Wild-type, *vtc2-4*, and *vtc3-3* plants were grown on MS plates under low-light (40–60 μmol photons
551 m^{-2} s^{-1}) conditions for two weeks and then exposed to moderate-light stress (650 μmol photons m^{-2} s
552 $^{-1}$) for 24 h. (A) Ascorbate oxidation by ascorbate peroxidase (APX) and its recycling through
553 monodehydroascorbate reductase (MDAR) and dehydroascorbate reductase (DHAR). (B) Total
554 ascorbate content (sum of ASC and DHA contents). (C) Total glutathione content (sum of GSH and
555 GSSG contents). (D) APX activity. (E) MDAR activity. (F) DHAR activity. Data are presented as the
556 mean ± SE of three or four biological replicates. Different letters indicate significant differences ($P <$
557 0.05, two-way ANOVA followed by Tukey–Kramer test). ASC, reduced ascorbate; DHA,
558 dehydroascorbate; FW, fresh weight; GSH, reduced glutathione; GSSG, oxidized glutathione.
559
560 **Figure 3** Transcriptomic changes in *vtc2-4* and *vtc3-3*
561 Wild-type, *vtc2-4*, and *vtc3-3* plants were grown on MS plates under low-light (40–60 μmol photons
562 m^{-2} s^{-1}) conditions for two weeks and then incubated in darkness for two days (to decline ascorbate
563 pool size), followed by a 6-hour exposure to light (100 μmol photons m^{-2} s^{-1}). From the triplicate data,
564 we selected the genes whose expression was significantly up-regulated (false discovery rate < 0.05)
565 in *vtc2-4* or *vtc3-3* compared to the wild-type plants. (A, B) The Venn diagrams show the overlap
566 between sets of genes upregulated (A) or downregulated (B) in *vtc2-4* and *vtc3-3*. (C) Gene ontology
567 enrichment analysis (biological process) of 12 genes whose expression was upregulated in *vtc3-3*
568 compared to the wild-type plants. (C) Gene ontology (GO) terms enriched in genes whose expression
569 was specifically promoted in *vtc3-3*. BG, background; Ref, reference.
570
571 **Figure 4** Phenotypes and ascorbate profiles of *vtc2-4 vtc3-3* double mutants
572 Wild-type, *vtc2-4*, *vtc3-3*, and *vtc2-4 vtc3-3* plants were grown in soil under low-light (40–60 μmol
573 photons m^{-2} s^{-1}) conditions for three weeks. Fully expanded leaves were used for ascorbate
574 measurements. (A) Representative phenotypes of plants. (B, C) Box plots illustrate fresh weights (B)
575 and the rosette area (C). Horizontal bars and cross marks within the box represent median and mean
576 values from 12 biological replicates, respectively, with boxes representing the 25th and 75th
577 percentiles. The outer error bars (whiskers) represent maximum and minimum values. There was no
578 significant difference between genotypes (one-way ANOVA). (D) Total ascorbate content (sum of

579 ASC and DHA contents). Data are presented as the mean ± SE of five biological replicates. Different
580 letters indicate significant differences ($P < 0.05$, one-way ANOVA followed by Tukey–Kramer test).
581 ASC, reduced ascorbate; DHA, dehydroascorbate; FW, fresh weight.
582
583 **Figure 5** Sensitivity of *vtc2-4 vtc3-3* double mutants to high-light stress
584 Wild-type, *vtc2-4*, *vtc3-3*, and *vtc2-4 vtc3-3* plants were grown in soil under low-light (40–60 μmol
585 photons m^{-2} s^{-1}) conditions for three weeks and then exposed to high-light stress (1,500 μmol photons
586 m^{-2} s^{-1}) for 24 h. (A) Representative phenotypes of plants before and after high-light stress. (B) Box
587 plots illustrate lesion area (% of whole rosette area). The data were obtained from nine plants per
588 genotype in three independent experiments. As wild-type plants showed no lesions, lesion area
589 analysis was not performed. Horizontal bars and cross marks within the box represent median and
590 mean values from five biological replicates, respectively, with boxes representing the 25th and 75th
591 percentiles. The outer error bars (whiskers) and diamonds represent the maximum and minimum
592 values, and an outlier, respectively. Different letters indicate significant differences ($P < 0.05$, one-
593 way ANOVA followed by Tukey–Kramer test). (C) The maximum quantum yield of photosystem II
594 (F_v/F_m) before and after high-light stress. Significant differences between genotypes (one-way
595 ANOVA followed by Tukey–Kramer test): $^{*}P < 0.05$, $^{**}P < 0.01$.
596
597 **Figure 6** Ascorbate profiles in *vtc2-4 vtc3-3* under high- or moderate-light stress
598 Wild-type, *vtc2-4*, *vtc3-3*, and *vtc2-4 vtc3-3* plants were grown in soil under low-light (40–60 μmol
599 photons m^{-2} s^{-1}) conditions for three weeks and then exposed to high-light stress (1,500 μmol photons
600 m^{-2} s^{-1}) for 24 h (A, B), or to moderate-light stress (750 μmol photons m^{-2} s^{-1}) for 48 h (C, D). Fully
601 expanded leaves were used for ascorbate measurements. (A, C) Total ascorbate content (sum of ASC
602 and DHA contents). Data are presented as the mean ± SE of three or four biological replicates.
603 Significant differences between data before and after light stress for each genotype (one-way-ANOVA
604 with Dunnett's post hoc test for total content): $P^{*} < 0.05$, $^{**}P < 0.01$, compared to the values of 0 h.
605 (B, D) The amounts of ascorbate increase from before to after high- or moderate-light exposure (24 or
606 48 h, respectively). Data are presented as the mean ± SE of three or four biological replicates. Different
607 letters indicate significant differences ($P < 0.05$, one-way ANOVA followed by Tukey–Kramer test).
608 ASC, reduced ascorbate; DHA, dehydroascorbate; FW, fresh weight; HL, high light; ML, moderate
609 light; n.s., not significant.
610
611 **Figure 7** Non-photochemical quenching in *vtc2-4 vtc3-3* before and after high-light stress

Wild-type, *vtc2-4*, *vtc3-3*, and *vtc2-4 vtc3-3* plants were grown in soil under low-light (40–60 µmol photons m^{-2} s^{-1}) conditions for three weeks and then exposed to high-light stress (1,500 µmol photons m^{-2} s^{-1}) for 24 h. (A, B) Non-photochemical quenching (NPQ) induction upon the onset of actinic light (90 µmol photons m^{-2} s^{-1}) before (A) and after (B) stress. Data are presented as the mean ± SE of three or four biological replicates. The red triangles indicate the data points used for statistical analysis (C, D). (C, D) Box plots illustrate NPQ data before (C) and after (D) stress, corresponding to the areas outlined with red dashed lines in (A) and (B), respectively. Horizontal bars and cross marks within the box represent median and mean values from 12 biological replicates, respectively, with boxes representing the 25th and 75th percentiles. The outer error bars (whiskers) represent maximum and minimum values. Different letters indicate significant differences ($P < 0.05$, one-way ANOVA followed by Tukey–Kramer test).

Supplementary Data

Supplementary Figure S1 Expression stability of the reference gene *Actin2* across different genotypes and treatment conditions

Supplementary Figure S2 Expression of *VTC2* and *VTC3* in *vtc* mutant lines

Supplementary Figure S3 Ascorbate treatment alleviates light stress-induced cell death in the *vtc2-4 vtc3-3* double mutant

Supplementary Table S1 List of primers used

Supplementary Table S2 List of genes whose expression is altered in *vtc* mutants and gene ontology enrichment analysis

Author Contributions

YT, TM, and TI: conceptualization; YT, TM, and TI: methodology; YT, and TM: formal analysis; YT, TM, KA, HN, AH, and TI: investigation; YT, and TM: data curation; YT, and TM: writing - original draft; KA, HN, AH, and TI: writing - review & editing; TM: visualization; TM, TI: supervision; TM, TI: funding acquisition

Conflicts of Interest

The authors declare no conflict of interest.

Funding Statement

This work was conducted as an SDGs Research Project of Shimane University (T.M.) and supported

by JSPS Bilateral Program Number JPJSBP120232302 (T.M.) and JSPS KAKENHI Grant Number 24K01680 (T.I.).

Data availability

The data underlying this article are available in the article and its online supplementary material. The raw and processed data of RNA-seq have been deposited in the Gene Expression Omnibus under accession number GSE293768.

Acknowledgments

We would like to thank Hiromi Ueno, Reona Tanimura, and Natsumi Ito for their technical assistance.

References

Aarabi F, Ghigi A, Wijesingha Ahchige M, Bulut M, Geigenberger P, Neuhaus HE, Sampathkumar A, Alseekh S, Fernie AR. 2023. Genome-Wide Association Study unveils ascorbate regulation by PAS/LOV PROTEIN during high light acclimation. Plant Physiology doi: 10.1093/plphys/kiad323.

Asada K. 1999. THE WATER-WATER CYCLE IN CHLOROPLASTS: Scavenging of active oxygens and dissipation of excess photons. Annual Review of Plant Physiology and Plant molecular biology **50**, 601–639.

Baker NR. 2008. Chlorophyll fluorescence: a probe of photosynthesis in vivo. Annual Review of Plant Biology **59**, 89–113.

Barth C, Gouzd ZA, Steele HP, Imperio RM. 2010. A mutation in GDP-mannose pyrophosphorylase causes conditional hypersensitivity to ammonium, resulting in Arabidopsis root growth inhibition, altered ammonium metabolism, and hormone homeostasis. Journal of experimental botany **61**, 379–394.

Bournonville C, Mori K, Deslous P, *et al.* 2023. Blue light promotes ascorbate synthesis by deactivating the PAS/LOV photoreceptor that inhibits GDP-L-galactose phosphorylase. The Plant Cell **35**, 2615–2634.

Bulley SM, Rassam M, Hoser D, Otto W, Schünemann N, Wright M, MacRae E, Gleave A, Laing W. 2009. Gene expression studies in kiwifruit and gene over-expression in Arabidopsis indicates that

675 GDP-L-galactose guanyltransferase is a major control point of vitamin C biosynthesis. Journal of
676 Experimental Botany **60**, 765–778.

677 **Bulley S, Wright M, Rommens C, *et al.*** 2012. Enhancing ascorbate in fruits and tubers through over-
678 expression of the L-galactose pathway gene GDP-L-galactose phosphorylase. Plant Biotechnology
679 Journal **10**, 390–397.

680 **Conklin PL, DePaolo D, Wintle B, Schatz C, Buckenmeyer G**. 2013. Identification of Arabidopsis
681 VTC3 as a putative and unique dual function protein kinase::protein phosphatase involved in the
682 regulation of the ascorbic acid pool in plants. Journal of Experimental Botany **64**, 2793–2804.

683 **Conklin PL, Gatzek S, Wheeler GL, Dowdle J, Raymond MJ, Rolinski S, Isupov M, Littlechild**
684 **JA, Smirnoff N**. 2006. *Arabidopsis thaliana VTC4* encodes L-galactose-1-P phosphatase, a plant
685 ascorbic acid biosynthetic enzyme. The Journal of Biological Chemistry **281**, 15662–15670.

686 **Conklin PL, Norris SR, Wheeler GL, Williams EH, Smirnoff N, Last RL**. 1999. Genetic evidence
687 for the role of GDP-mannose in plant ascorbic acid (vitamin C) biosynthesis. Proceedings of the
688 National Academy of Sciences of the United States of America **96**, 4198–4203.

689 **Conklin PL, Saracco SA, Norris SR, Last RL**. 2000. Identification of ascorbic acid-deficient
690 *Arabidopsis thaliana* mutants. Genetics **154**, 847–856.

691 **Dowdle J, Ishikawa T, Gatzek S, Rolinski S, Smirnoff N**. 2007. Two genes in *Arabidopsis thaliana*
692 encoding GDP-L-galactose phosphorylase are required for ascorbate biosynthesis and seedling
693 viability. The Plant Journal **52**, 673–689.

694 **Fenech M, Amorim-Silva V, Esteban Del Valle A, Arnaud D, Ruiz-Lopez N, Castillo AG,**
695 **Smirnoff N, Botella MA**. 2021. The role of GDP-l-galactose phosphorylase in the control of ascorbate
696 biosynthesis. Plant Physiology **185**, 1574–1594.

697 **Foyer CH, Halliwell B**. 1977. Purification and properties of dehydroascorbate reductase from spinach
698 leaves. Phytochemistry **16**, 1347–1350.

699 **Hamada T, Maruta T**. 2024. Measurements of ascorbate and dehydroascorbate in plants using high-
700 performance liquid chromatography. Methods in Molecular Biology (Clifton, N.J.) **2798**, 131–139.

701 **Hamada A, Tanaka Y, Ishikawa T, Maruta T**. 2023. Chloroplast dehydroascorbate reductase and

702 glutathione cooperatively determine the capacity for ascorbate accumulation under photooxidative
703 stress conditions. The Plant Journal **114**, 68–82.

704 **Hossain MA, Asada K**. 1985. Monodehydroascorbate reductase from cucumber is a flavin adenine
705 dinucleotide enzyme. The Journal of Biological Chemistry **260**, 12920–12926.

706 **Ishida T, Tanaka Y, Maruta T, Ishikawa T**. 2024. The D-mannose/L-galactose pathway plays a
707 predominant role in ascorbate biosynthesis in the liverwort *Marchantia polymorpha* but is not
708 regulated by light and oxidative stress. The Plant Journal **117**, 805–817.

709 **Iwagami T, Ogawa T, Ishikawa T, Maruta T**. 2022. Activation of ascorbate metabolism by nitrogen
710 starvation and its physiological impacts in Arabidopsis thaliana. Bioscience, Biotechnology, and
711 Biochemistry **86**, 476–489.

712 **Jander G, Norris SR, Rounsley SD, Bush DF, Levin IM, Last RL**. 2002. Arabidopsis map-based
713 cloning in the post-genome era. Plant Physiology **129**, 440–450.

714 **Kameoka T, Okayasu T, Kikuraku K, Ogawa T, Sawa Y, Yamamoto H, Ishikawa T, Maruta T**.
715 2021. Cooperation of chloroplast ascorbate peroxidases and proton gradient regulation 5 is critical for
716 protecting Arabidopsis plants from photo-oxidative stress. The Plant Journal **107**, 876–892.

717 **Laing WA, Martínez-Sánchez M, Wright MA, *et al.*** 2015. An upstream open reading frame is
718 essential for feedback regulation of ascorbate biosynthesis in Arabidopsis. The Plant Cell **27**, 772–786.

719 **Laing WA, Wright MA, Cooney J, Bulley SM**. 2007. The missing step of the L-galactose pathway
720 of ascorbate biosynthesis in plants, an L-galactose guanyltransferase, increases leaf ascorbate content.
721 Proceedings of the National Academy of Sciences of the United States of America **104**, 9534–9539.

722 **Lim B, Smirnoff N, Cobbett CS, Golz JF**. 2016. Ascorbate-deficient *vtc2* mutants in Arabidopsis do
723 not exhibit decreased growth. Frontiers in Plant Science **7**, 1025.

724 **Linster CL, Gomez TA, Christensen KC, Adler LN, Young BD, Brenner C, Clarke SG**. 2007.
725 Arabidopsis *VTC2* encodes a GDP-L-galactose phosphorylase, the last unknown enzyme in the
726 Smirnoff-Wheeler pathway to ascorbic acid in plants. The Journal of Biological Chemistry **282**,
727 18879–18885.

728 **Lorence A, Chevone BI, Mendes P, Nessler CL**. 2004. Myo-inositol oxygenase offers a possible

729 entry point into plant ascorbate biosynthesis. Plant Physiology **134**, 1200-1205.

730 **Maruta T**. 2022. How does light facilitate vitamin C biosynthesis in leaves? Bioscience,
731 Biotechnology, and Biochemistry **86**, 1173–1182.

732 **Maruta T, Sawa Y, Shigeoka S, Ishikawa T**. 2016. Diversity and evolution of ascorbate peroxidase
733 functions in chloroplasts: More than just a classical antioxidant enzyme? Plant & Cell Physiology **57**,
734 1377–1386.

735 **Maruta T, Tanaka Y, Yamamoto K, Ishida T, Hamada A, Ishikawa T**. 2024. Evolutionary insights
736 into strategy shifts for the safe and effective accumulation of ascorbate in plants. Journal of
737 Experimental Botany **75**, 2664–2681.

738 **Mittler R, Zandalinas SI, Fichman Y, Van Breusegem F**. 2022. Reactive oxygen species signalling
739 in plant stress responses. Nature Reviews. Molecular Cell Biology **23**, 663–679.

740 **Müller-Moulé P, Golan T, Niyogi KK**. 2004. Ascorbate-deficient mutants of Arabidopsis grow in
741 high light despite chronic photooxidative stress. Plant Physiology **134**, 1163–1172.

742 **Noctor G, Mhamdi A, Foyer CH**. 2016. Oxidative stress and antioxidative systems: recipes for
743 successful data collection and interpretation. Plant, Cell & Environment **39**, 1140–1160.

744 **Ogura Y, Komatsu A, Zikihara K, Nanjo T, Tokutomi S, Wada M, Kiyosue T**. 2008. Blue light
745 diminishes interaction of PAS/LOV proteins, putative blue light receptors in *Arabidopsis thaliana*,
746 with their interacting partners. Journal of Plant Research **121**, 97–105.

747 **Pastori GM, Kiddle G, Antoniw J, Bernard S, Veljovic-Jovanovic S, Verrier PJ, Noctor G, Foyer**
748 **CH**. 2003. Leaf vitamin C contents modulate plant defense transcripts and regulate genes that control
749 development through hormone signaling. The Plant Cell **15**, 939–951.

750 **Plumb W, Townsend AJ, Rasool B, Alomrani S, Razak N, Karpinska B, Ruban AV, Foyer CH**.
751 2018. Ascorbate-mediated regulation of growth, photoprotection, and photoinhibition in *Arabidopsis*
752 *thaliana*. Journal of Experimental Botany **69**, 2823–2835.

753 **Rahantaniaina M-S, Li S, Chatel-Innocenti G, Tuzet A, Issakidis-Bourguet E, Mhamdi A, Noctor**
754 **G**. 2017. Cytosolic and chloroplastic DHARs cooperate in oxidative stress-driven activation of the
755 salicylic acid pathway. Plant Physiology **174**, 956–971.

Shigeoka S, Ishikawa T, Tamoi M, Miyagawa Y, Takeda T, Yabuta Y, Yoshimura K. 2002. Regulation and function of ascorbate peroxidase isoenzymes. Journal of Experimental Botany **53**, 1305–1319.

Smirnoff N. 2018. Ascorbic acid metabolism and functions: A comparison of plants and mammals. Free Radical Biology and Medicine **122**, 116–129.

Sodeyama T, Nishikawa H, Harai K, Takeshima D, Sawa Y, Maruta T, Ishikawa T. 2021. The d-mannose/l-galactose pathway is the dominant ascorbate biosynthetic route in the moss *Physcomitrium patens*. The Plant Journal **107**, 1724–1738.

Tanaka M, Takahashi R, Hamada A, Terai Y, Ogawa T, Sawa Y, Ishikawa T, Maruta T. 2021. Distribution and functions of monodehydroascorbate reductases in plants: Comprehensive reverse genetic analysis of *Arabidopsis thaliana* Enzymes. Antioxidants **10**.

Terai Y, Ueno H, Ogawa T, Sawa Y, Miyagi A, Kawai-Yamada M, Ishikawa T, Maruta T. 2020. Dehydroascorbate reductases and glutathione set a threshold for high-light-induced ascorbate accumulation. Plant Physiology **183**, 112–122.

Tian T, Liu Y, Yan H, You Q, Yi X, Du Z, Xu W, Su Z. 2017. agriGO v2.0: a GO analysis toolkit for the agricultural community, 2017 update. Nucleic Acids Research **45**, W122–W129.

Torabinejad J, Donahue JL, Gunesekera BN, Allen-Daniels MJ, Gillaspy GE. 2009. VTC4 is a bifunctional enzyme that affects myoinositol and ascorbate biosynthesis in plants. Plant Physiology **150**, 951–961.

Vidal-Meireles A, Neupert J, Zsigmond L, Rosado-Souza L, Kovács L, Nagy V, Galambos A, Fernie AR, Bock R, Tóth SZ. 2017. Regulation of ascorbate biosynthesis in green algae has evolved to enable rapid stress-induced response via the *VTC2* gene encoding GDP-l-galactose phosphorylase. The New Phytologist **214**, 668–681.

Wheeler GL, Jones MA, Smirnoff N. 1998. The biosynthetic pathway of vitamin C in higher plants. Nature **393**, 365–369.

Winkler BS, Orselli SM, Rex TS. 1994. The redox couple between glutathione and ascorbic acid: a chemical and physiological perspective. Free Radical Biology & Medicine **17**, 333–349.

Yabuta Y, Mieda T, Rapolu M, Nakamura A, Motoki T, Maruta T, Yoshimura K, Ishikawa T, Shigeoka S. 2007. Light regulation of ascorbate biosynthesis is dependent on the photosynthetic electron transport chain but independent of sugars in Arabidopsis. Journal of Experimental Botany **58**, 2661–2671.

Yoshimura K, Nakane T, Kume S, Shiomi Y, Maruta T, Ishikawa T, Shigeoka S. 2014. Transient expression analysis revealed the importance of VTC2 expression level in light/dark regulation of ascorbate biosynthesis in Arabidopsis. Bioscience, Biotechnology, and Biochemistry **78**, 60–66.

Zechmann B, Stumpe M, Mauch F. 2011. Immunocytochemical determination of the subcellular distribution of ascorbate in plants. Planta **233**, 1–12.

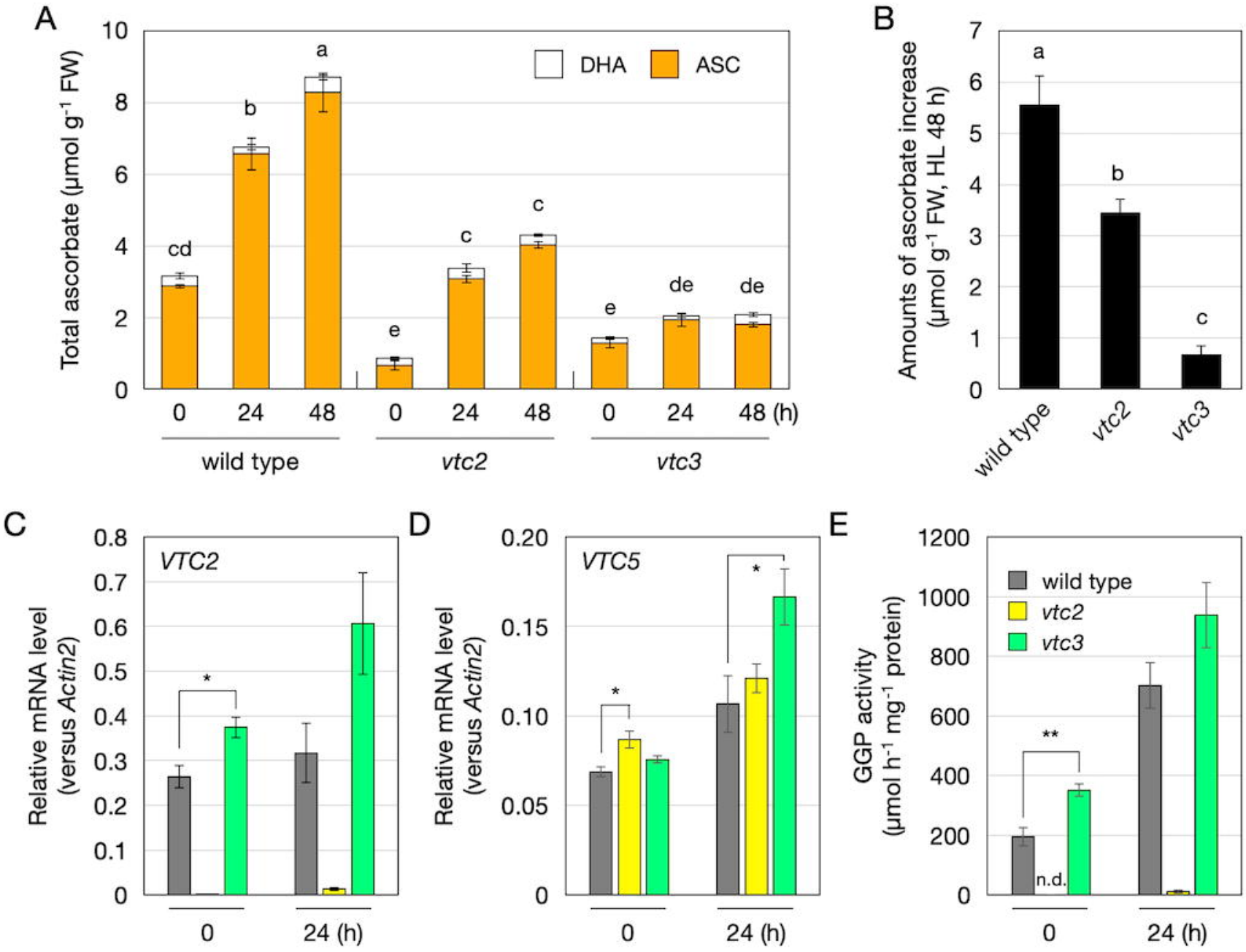

Tanaka & Maruta et al., Figure 1

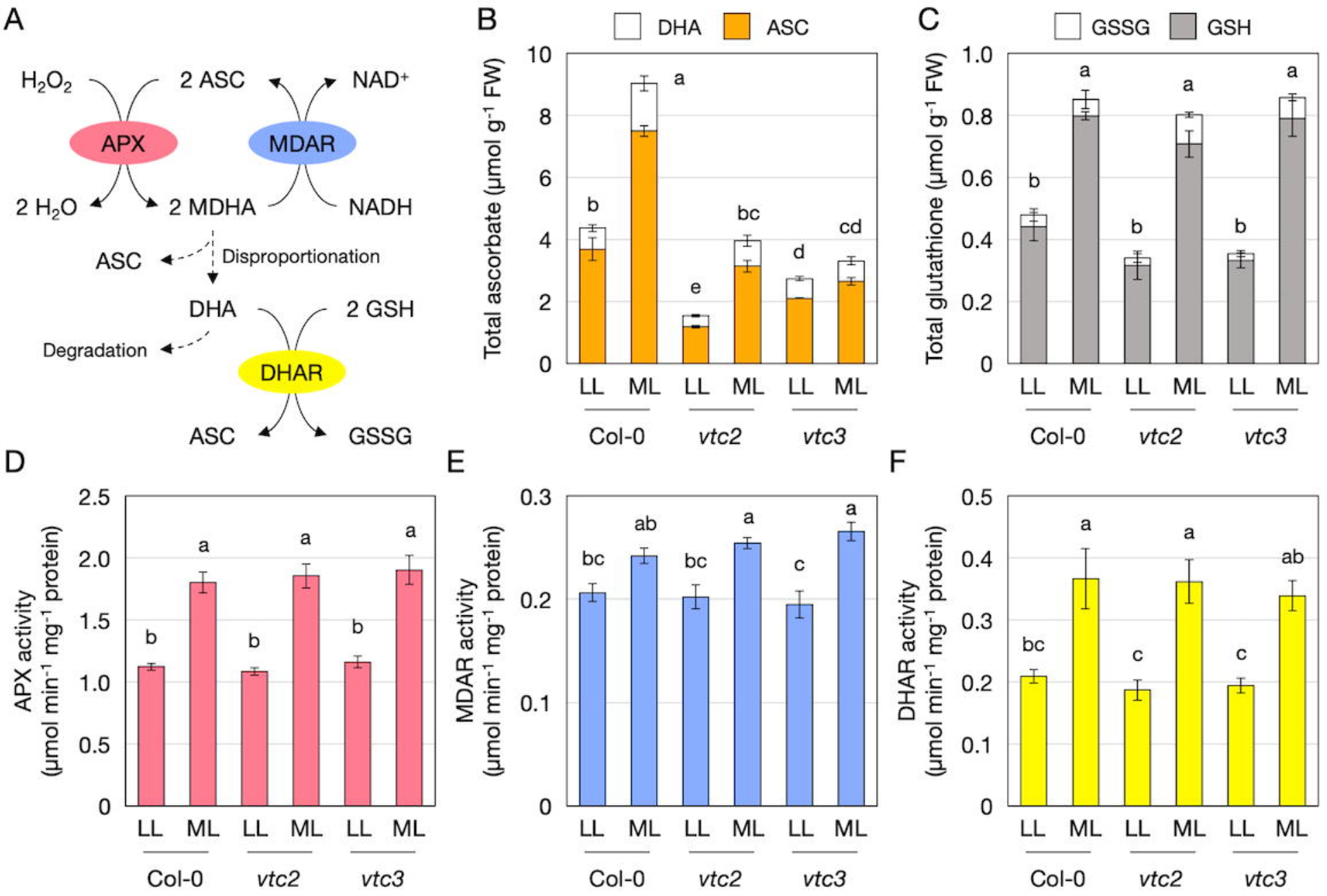

Tanaka & Maruta et al., Figure 2

A

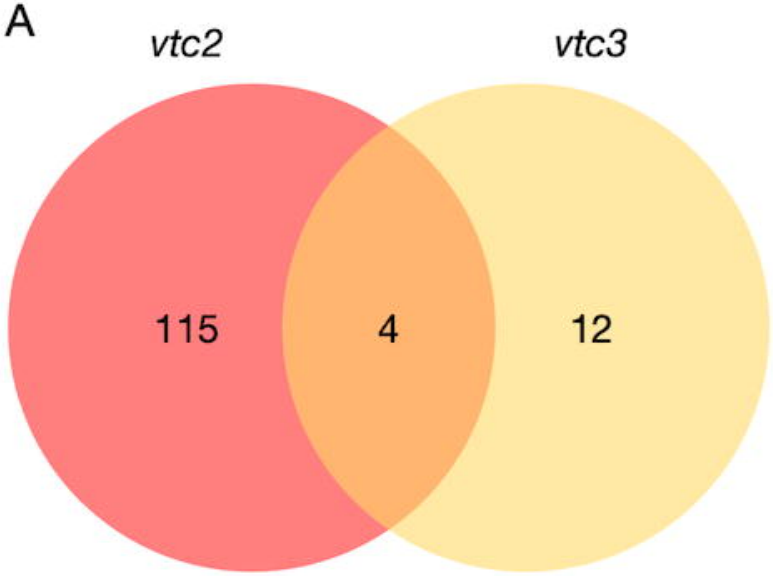

Upregulated genes vs wild type
(FDR *P* value < 0.05)

B

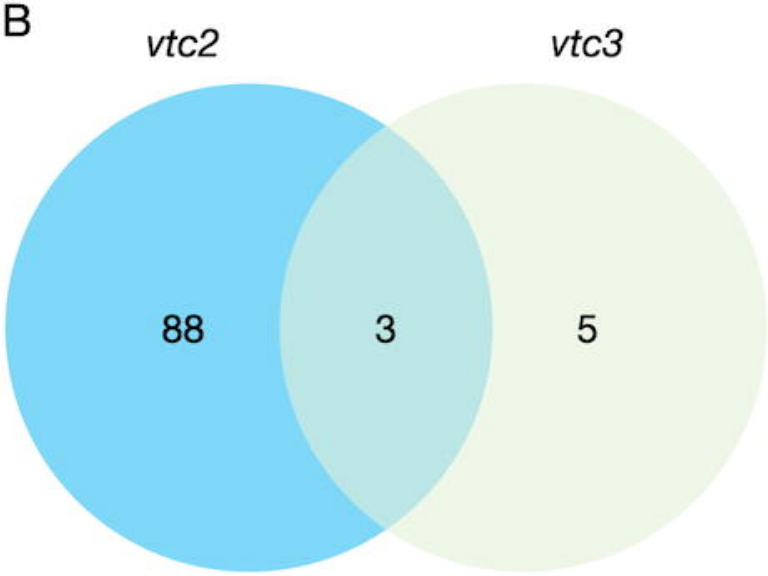

Downregulated genes vs wild type
(FDR *P* value < 0.05)

C

GO term	Description	Number in input list	Number in BG/Ref	*p*-value	FDR
GO:0006952	defense response	7	1566	9.80E-07	1.90E-05
GO:0050832	defense response to fungus	5	504	1.30E-06	1.90E-05
GO:0006950	response to stress	9	3506	1.10E-06	1.90E-05
GO:0098542	defense response to other organism	6	936	1.00E-06	1.90E-05
GO:0009620	response to fungus	5	573	2.40E-06	2.80E-05
GO:0043207	response to external biotic stimulus	6	1212	4.60E-06	3.80E-05
GO:0051707	response to other organism	6	1210	4.50E-06	3.80E-05
GO:0009607	response to biotic stimulus	6	1253	5.50E-06	4.00E-05
GO:0009605	response to external stimulus	6	1582	2.10E-05	0.00014
GO:0051704	multi-organism process	6	1631	2.50E-05	0.00015

Tanaka & Maruta et al., Figure 3

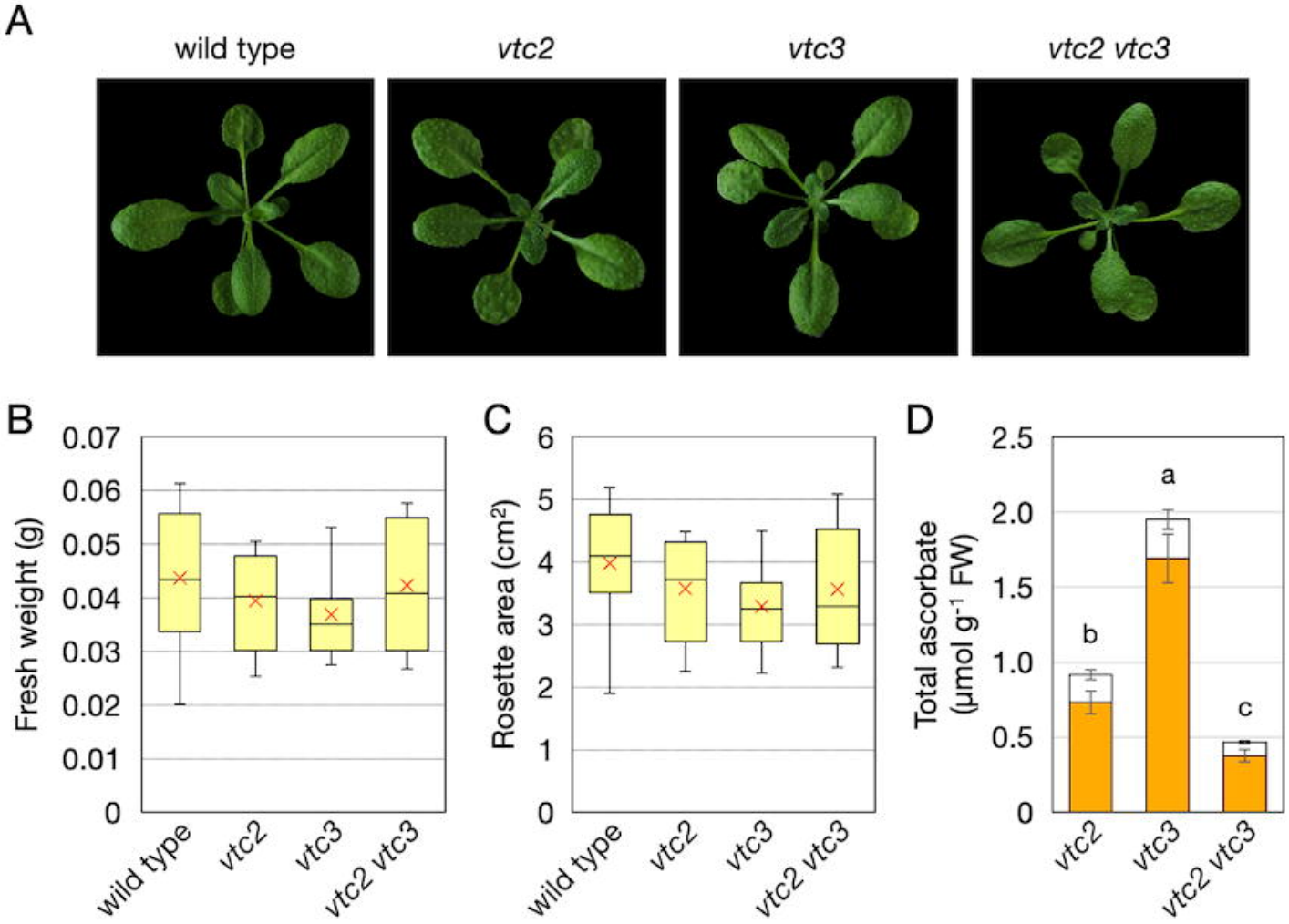

Tanaka & Maruta et al., Figure 4

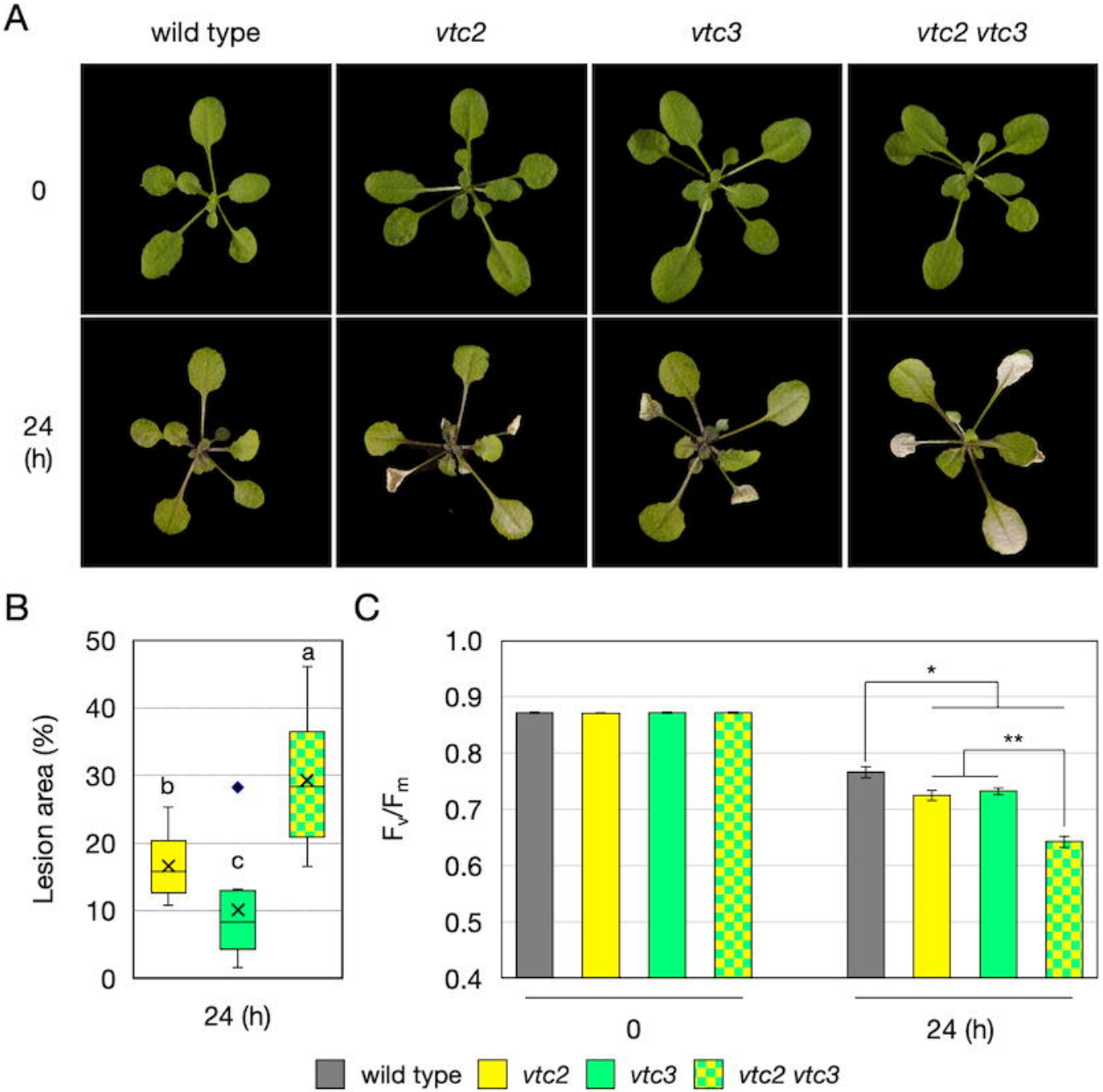

Tanaka & Maruta et al., Figure 5

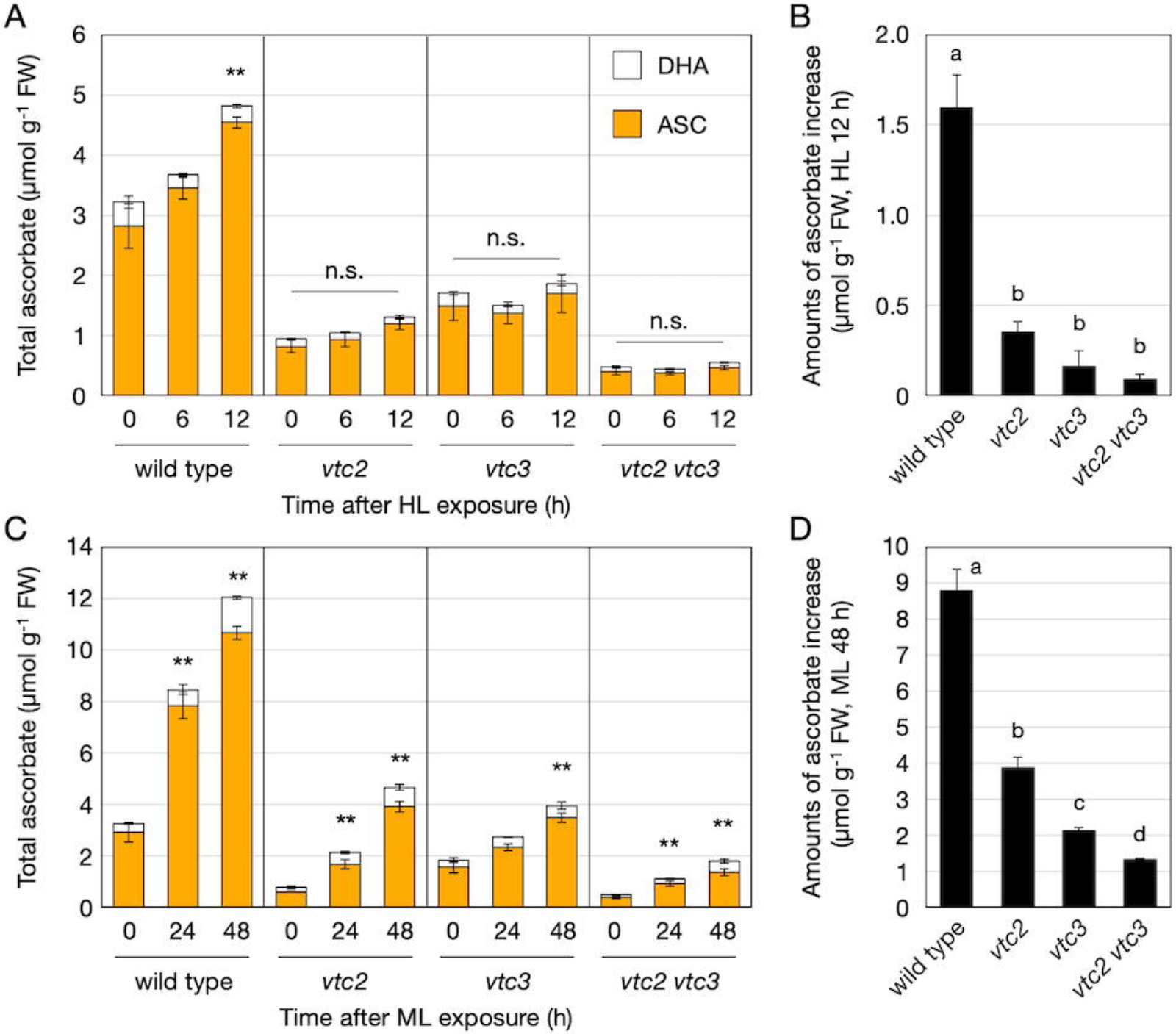

Tanaka & Maruta et al., Figure 6

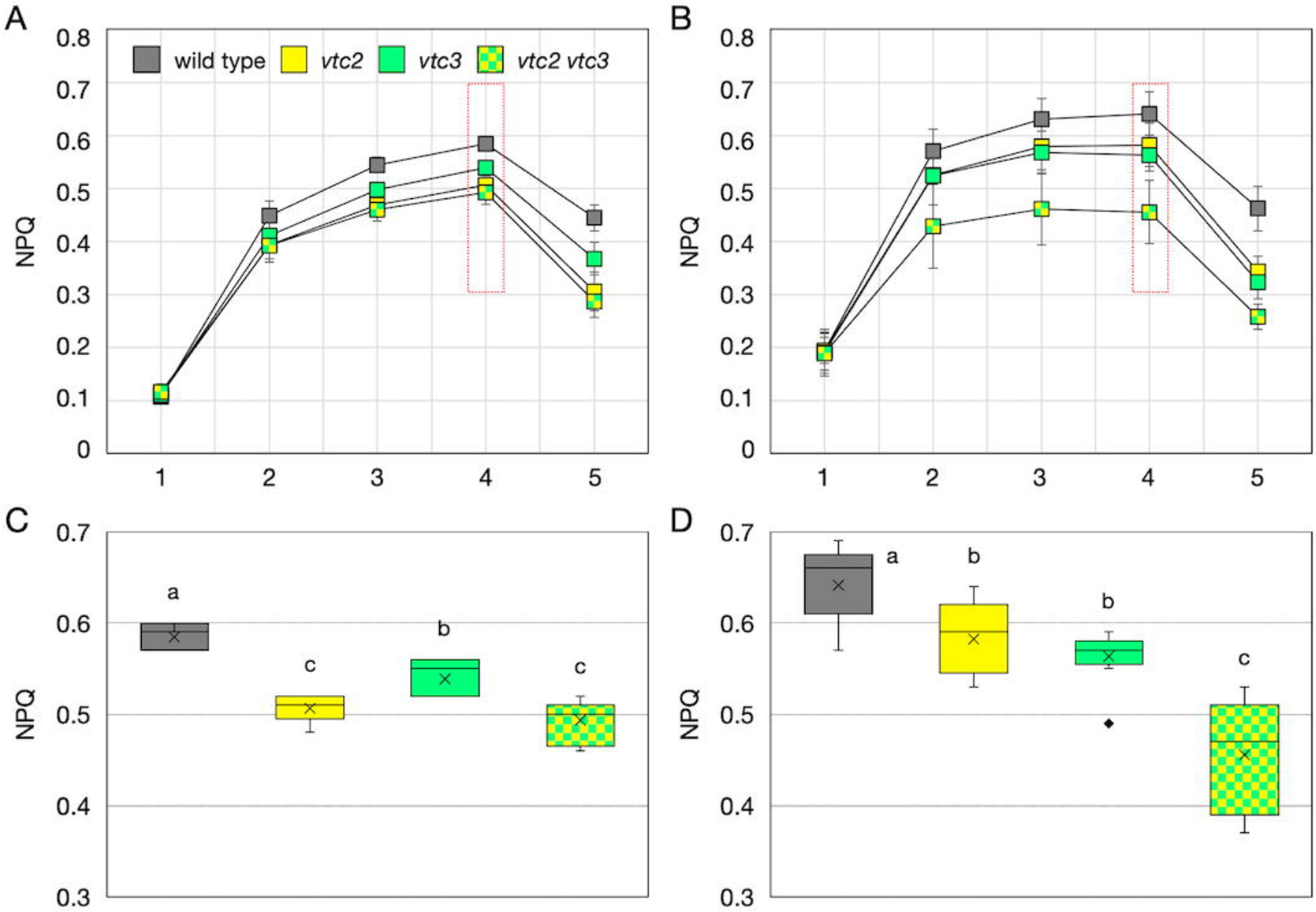

Tanaka & Maruta et al., Figure 7